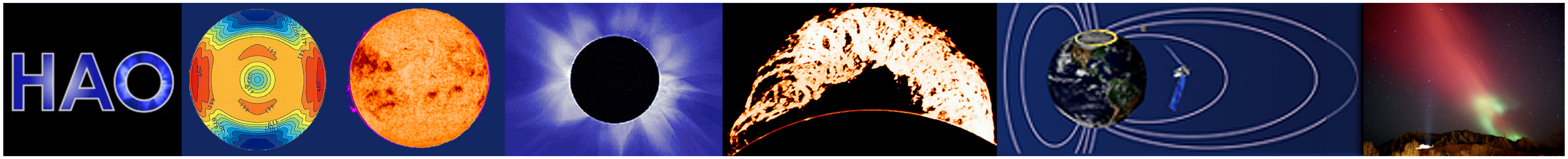

Differential Rotation and Emerging Flux in a Solar Convective Dynamo Simulation

Yuhong Fan and Fang Fang

NCAR

Work supported by NASA LWSCSW Grant NNX13AJ04A

PI: Nagi Mansour

Workshop on Sunspot Formation at NODITA, March 10, 2015

- Cyclic dynamo in a global implicit large-eddy anelastic MHD simulation of the solar convective envelope (Ghizaru et al 2010, Racine et al. 2011)

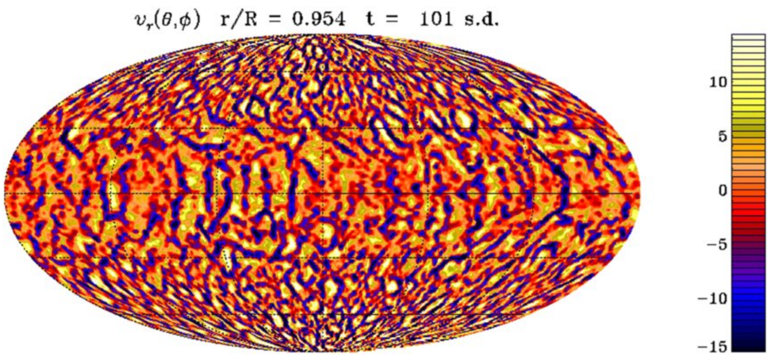

- Solar-like differential rotation with a shear tachocline layer.
- A strong and cyclic large-scale axisymmetric magnetic component undergoing regular polarity reversals at a period of 30 years
- Behaves like an $\alpha^2\Omega$ dynamo
- Convection maintained by an entropy gradient imposed by a Newtonian cooling term in the entropy equation.

Estimated $Co = 2\Omega/(u_{rms} 2\pi/\Delta r) \sim 6$

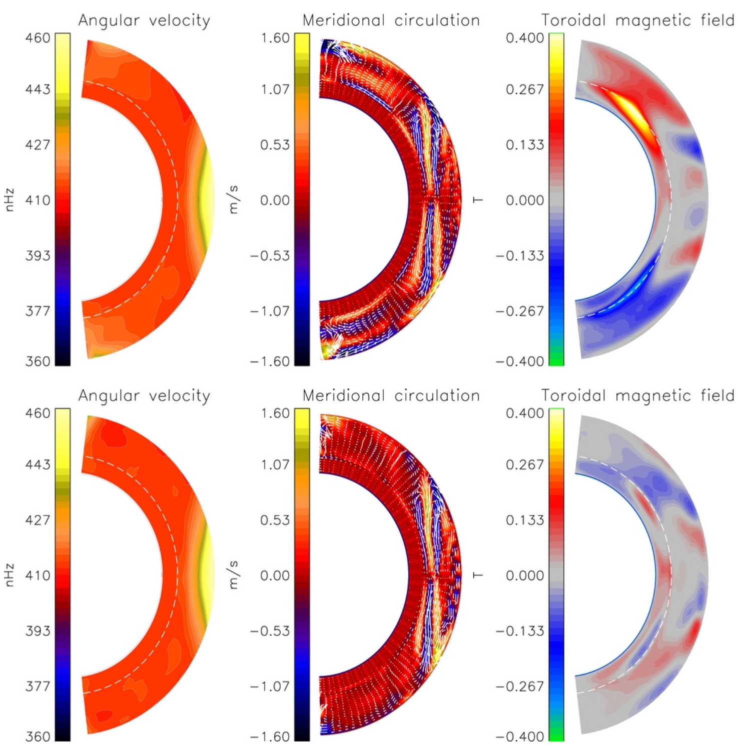

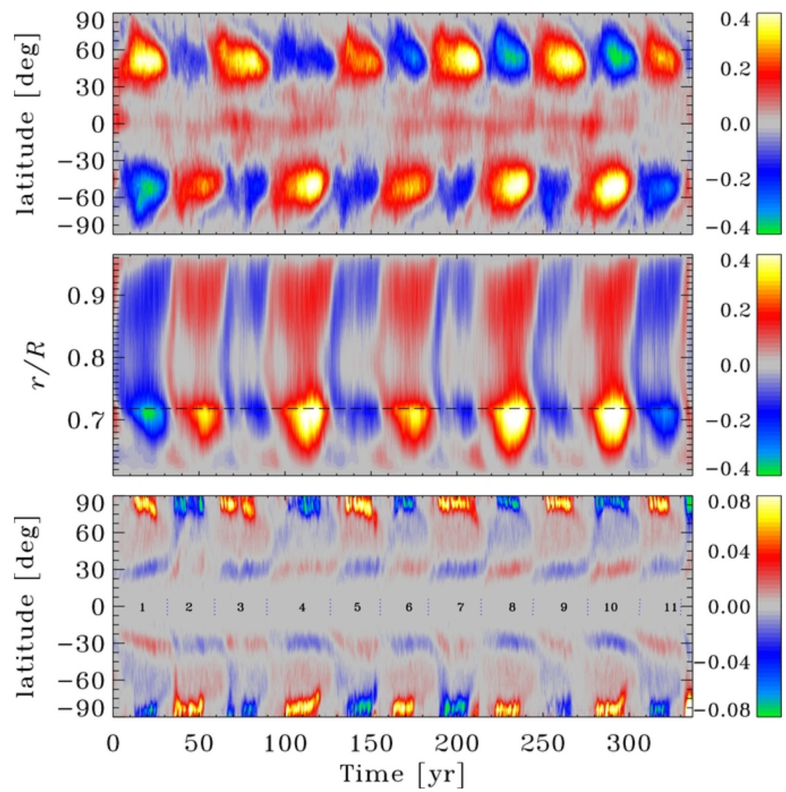

Global MHD simulations of turbulent dynamo in a fast rotating young sun with ASH

Nelson et al. (2011, 2013)

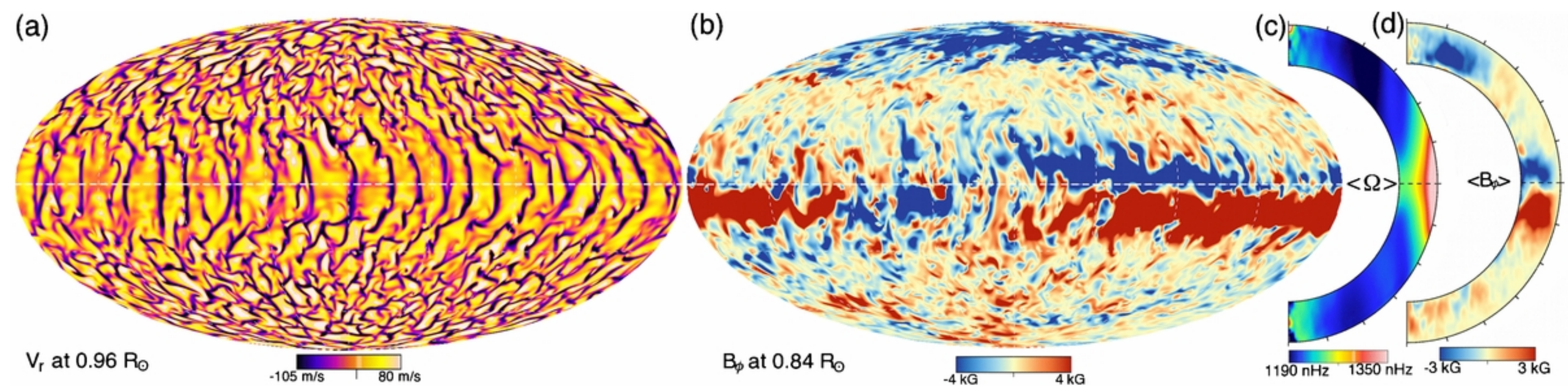

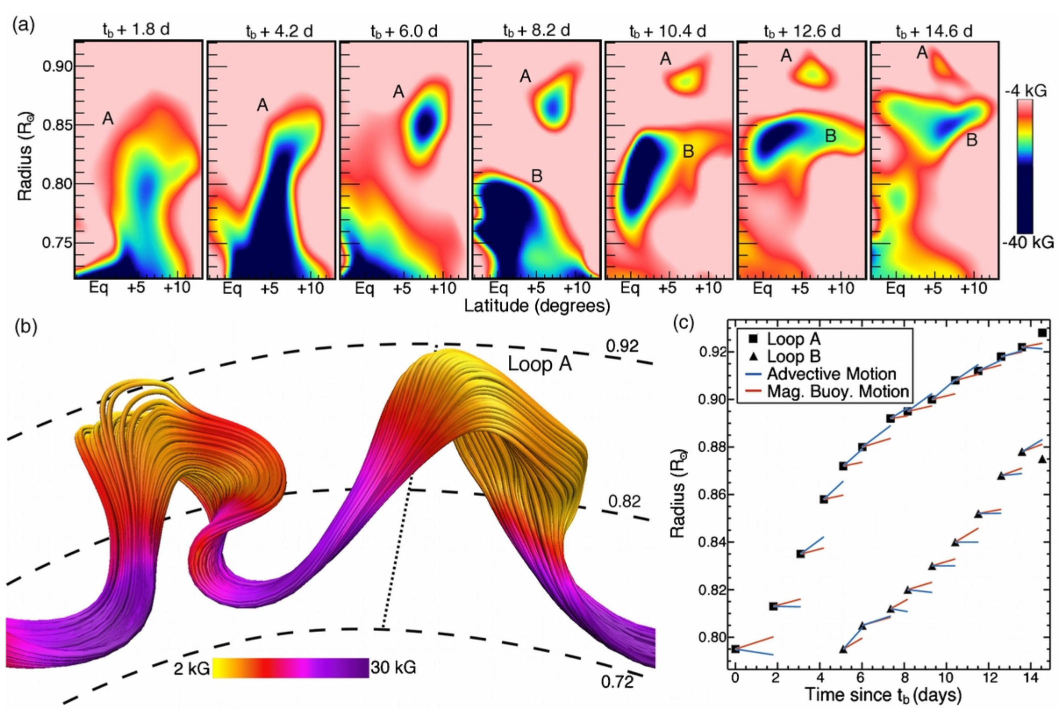

- Attains a differential rotation created by the interplay of convection, rotation and stratification.
- Produces large-scale toroidal magnetic structures that undergo cycles and reversals of global polarity.
- Forms buoyant magnetic loops from the strongest portions (>35kG) of the toroidal structures which rise from the base of the convection zone to above 0.9 R_s

- Regular magnetic cycles with equator-ward-propagating mean toroidal field in compressible MHD simulations of convective dynamo (Käpylä et al. 2012):

$$Co = 2\Omega/(u_{rms} 2\pi/\Delta r) = 7.6$$

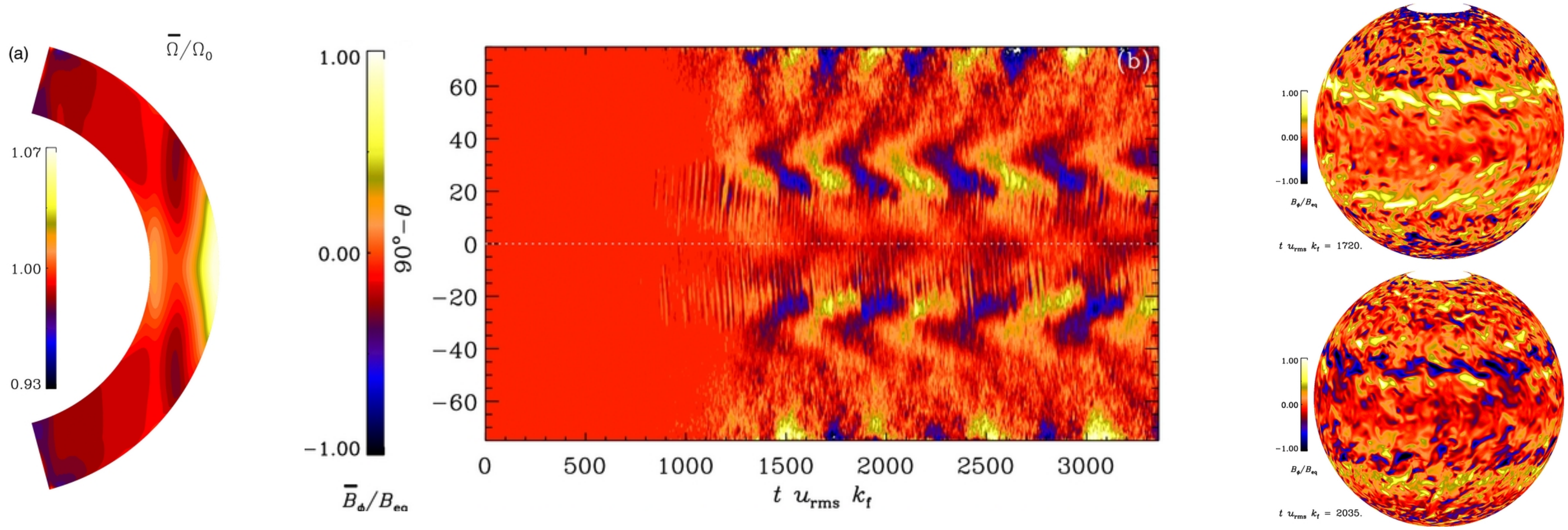

- Regular magnetic cycles with equator-ward-propagating mean toroidal field and grand minima in a rapidly rotating young sun (3 times solar rotation rate) from ASH global simulations (Augustson et al. 2013)

Estimating assuming $u_{rms} \sim 100\,ms^{-1}$: $Co = 2\Omega/(u_{rms} 2\pi/\Delta r) \sim 4.5$

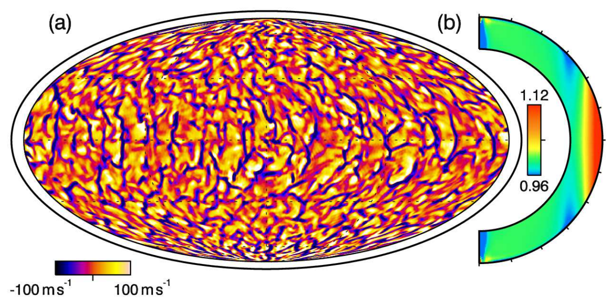

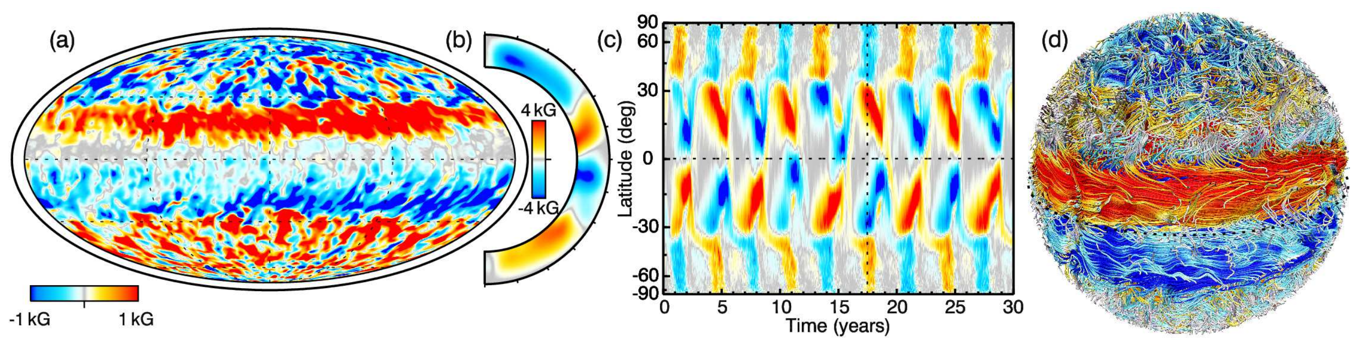

- Finite-difference Spherical Anelastic MHD (FSAM) code solves the following anelastic MHD equations in a partial spherical shell domain:

$$\nabla \cdot (\rho_0 \mathbf{v}) = 0,$$

$$\rho_0 \left[\frac{\partial \mathbf{v}}{\partial t} + (\mathbf{v} \cdot \nabla)\mathbf{v} \right] = 2\rho_0 \mathbf{v} \times \mathbf{\Omega} - \nabla p_1 + \rho_1 \mathbf{g} + \frac{1}{4\pi}(\nabla \times \mathbf{B}) \times \mathbf{B} + \nabla \cdot \mathcal{D}$$

$$\rho_0 T_0 \left[\frac{\partial s_1}{\partial t} + (\mathbf{v} \cdot \nabla)(s_0 + s_1) \right] = \nabla \cdot (K \rho_0 T_0 \nabla s_1) - (\mathcal{D} \cdot \nabla) \cdot \mathbf{v} + \frac{1}{4\pi} \eta (\nabla \times \mathbf{B})^2 - \nabla \cdot \mathbf{F}_{\mathrm{rad}}$$

$$\nabla \cdot \mathbf{B} = 0$$

$$\frac{\partial \mathbf{B}}{\partial t} = \nabla \times (\mathbf{v} \times \mathbf{B}) - \nabla \times (\eta \nabla \times \mathbf{B}),$$

$$\frac{\rho_1}{\rho_0} = \frac{p_1}{p_0} - \frac{T_1}{T_0},$$

$$\frac{s_1}{c_p} = \frac{T_1}{T_0} - \frac{\gamma - 1}{\gamma} \frac{p_1}{p_0},$$

where D is the viscous stress tensor, and $\mathbf{F}_{\mathrm{rad}}$ is the radiative diffusive heat flux:

$$\mathbf{F}_{\mathrm{rad}} = \frac{16 \sigma_s {T_0}^3}{3 \kappa \rho_0} \nabla T_0,$$

A convective dynamo simulation

(Fan and Fang 2014, ApJ, 789, 35)

- Simulation domain $r \in (0.722R_s, 0.971R_s)$, $\theta \in (\pi/2 - \pi/3, \pi/2 + \pi/3)$, $\phi \in (0, 2\pi)$
- Grid: $96 \times 512 \times 768$, horizontal res. at top boundary 2.8 Mm to 5.5 Mm, vertical res. 1.8 Mm
- $K = 3 \times 10^{13}\ cm^2 s^{-1}$, $\nu = 10^{12}\ cm^2 s^{-1}$, $\eta = 10^{12}\ cm^2 s^{-1}$, at top and all decrease with depth as $1/\sqrt{\rho}$
- Convection is driven by the radiative diffusive heat flux as a source term in the entropy equation:

$$\nabla \bullet \left(\mathbf{F}_{\mathbf{rad}}\right) = \nabla \bullet \left(\frac{16\sigma_s T_0^3}{3\kappa\rho_0} \nabla T_0\right)$$

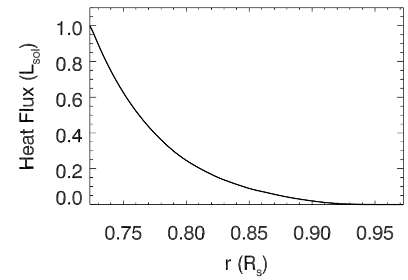

- The boundary condition for s_1:

at the bottom $\frac{\partial s_1}{\partial r} = 0$, and a latitudinal gradient is imposed: $\left(\frac{\partial s_1}{\partial \theta}\right) = \frac{ds_i(\theta)}{d\theta}$ where $s_i(\theta) = -\Delta s_i \cos\left(\frac{\theta - \pi/2}{\Delta\theta}\pi\right)$

at the top s_1 is held fixed, and s_1 is symmetric at the θ - boundaries

- The velocity boundary condition is non-penetrating and stress free at the and the top, bottom and θ−bondaries
- For the magnetic field: perfect conducting walls for the bottom and the θ−boundaries; radial field at the top boundary
- Angular rotation rate for the reference frame $\Omega = 2.7 \times 10^{-6}$ rad/s , net angular momentum relative to the reference frame is zero.

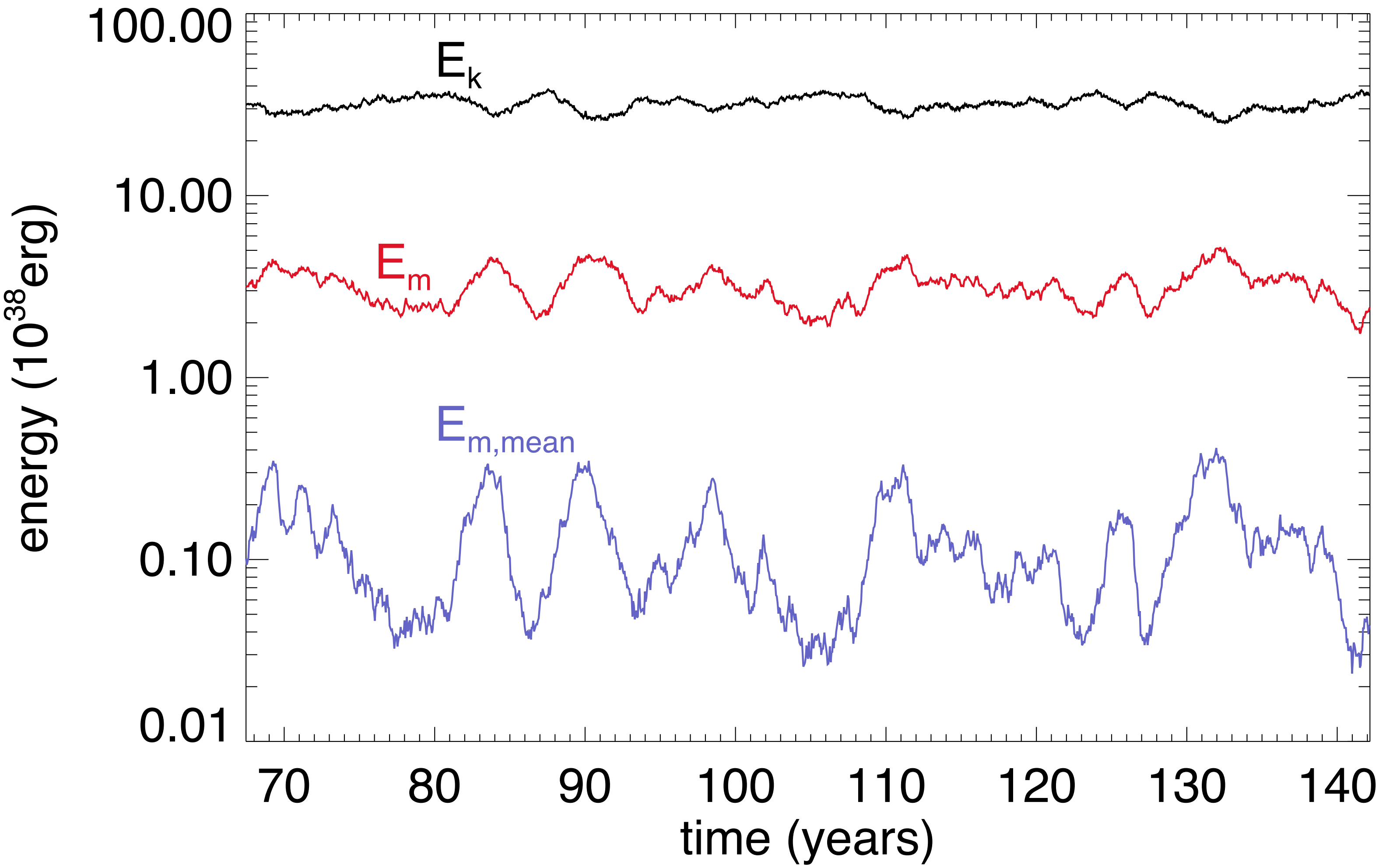

100.00
10.00
1.00
0.10
0.01
energy (10^{38}erg)
E_k
E_m
$E_{m,mean}$
70
80
90
100
110
120
130
140
time (years)

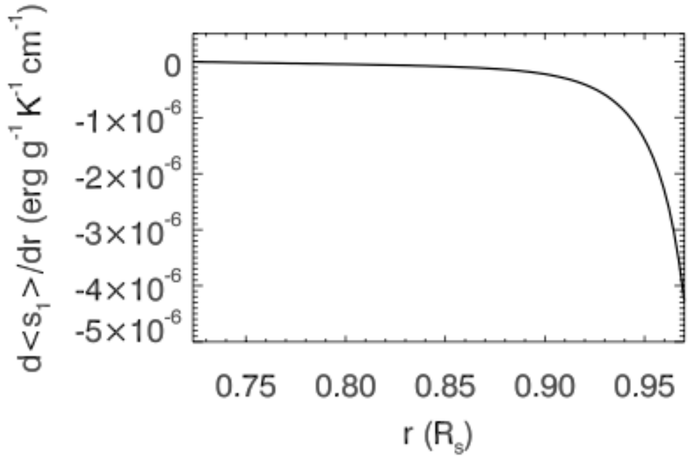

Consistent with Model S of JCD: the entropy gradient at $0.97R_s$ is ~10^{-5} erg g^{-1} K^{-1} cm^{-1}

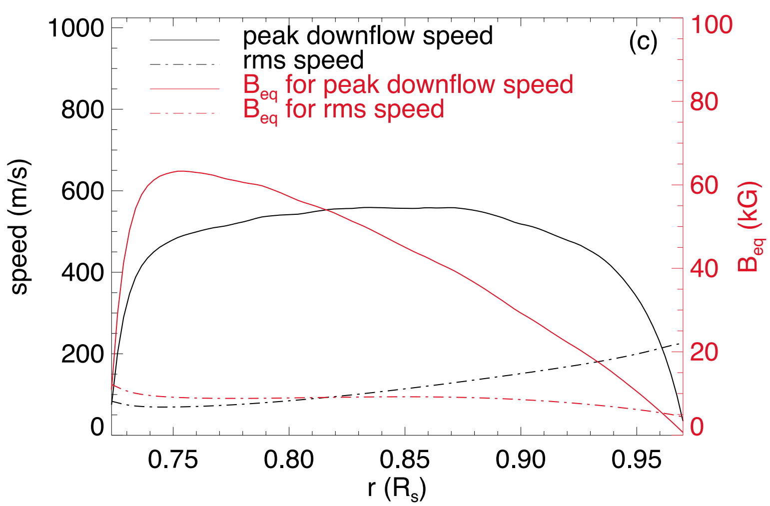

$\mathrm{Re} = u_{rms}/\nu k_f \approx$ 130 to 50 from bottom to top

$Co = 2\Omega/u_{rms,all}k_f \approx 1.3$, where $k_f = 2\pi/(r_o - r_i)$

$Ro = u_{rms,all}/\Omega l \approx 0.74$, where $l = H_p$ at bottom

Compared to Kapyla et al. (2012):

Re = 36

$Co = 7.6$

Our dynamo is in a much less rotationally constrained regime compared to Kapyla et al.(2012), Nelson et al. (2013), Augustson et al. (2013).

Compared to Ghizaru et al. (2010):
downflow speed 25 m/s vs. our 300 m/s at 0.954 R_s

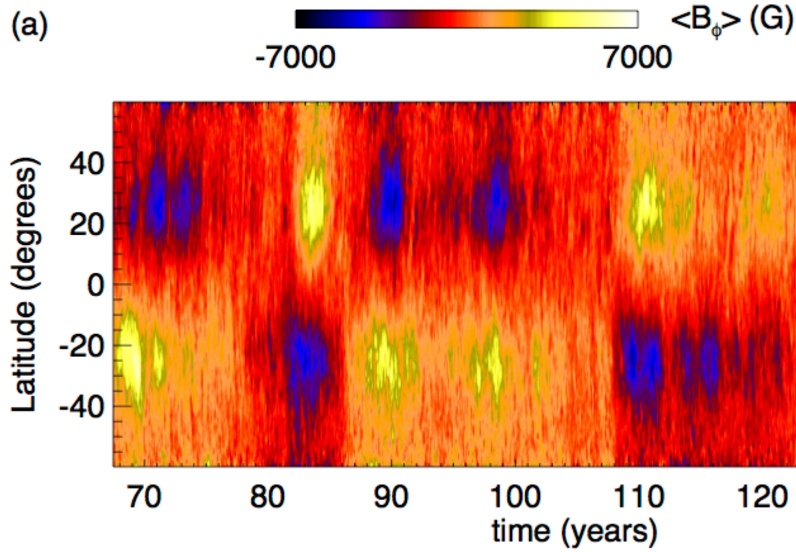

(a)
<B_φ> (G)
-7000
7000
Latitude (degrees)
40
20
0
-20
-40
70
80
90
100
110
120
130
140
time (years)

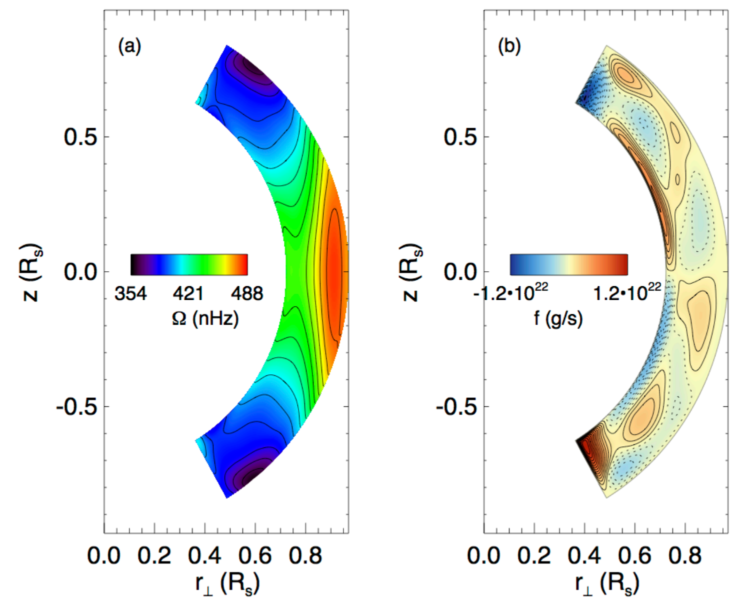

(a)
(b)
z (R_s)
0.5
0.0
-0.5
354
421
488
Ω (nHz)
-1.2•10^22
1.2•10^22
f (g/s)
0.0
0.2
0.4
0.6
0.8
r_⊥ (R_s)

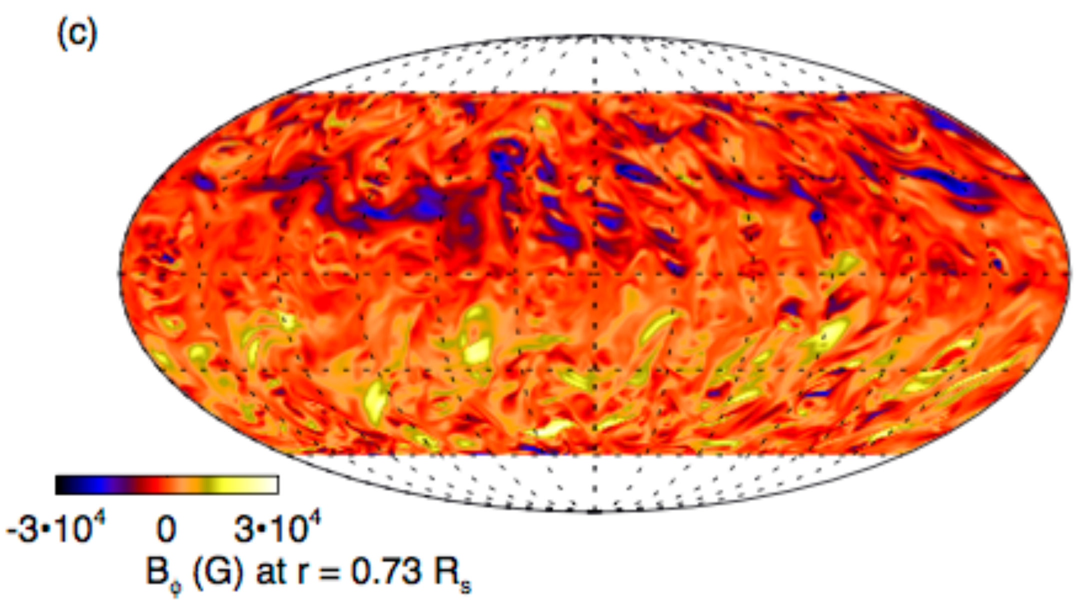

(c)
-3•10^4
0
3•10^4
B_φ (G) at r = 0.73 R_s

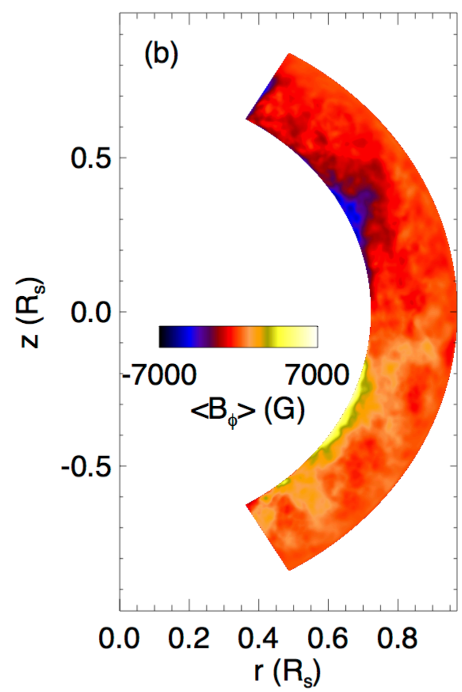

(b)
z (R_s)
0.5
0.0
-0.5
-7000
7000
<B_φ> (G)
0.0
0.2
0.4
0.6
0.8
r (R_s)

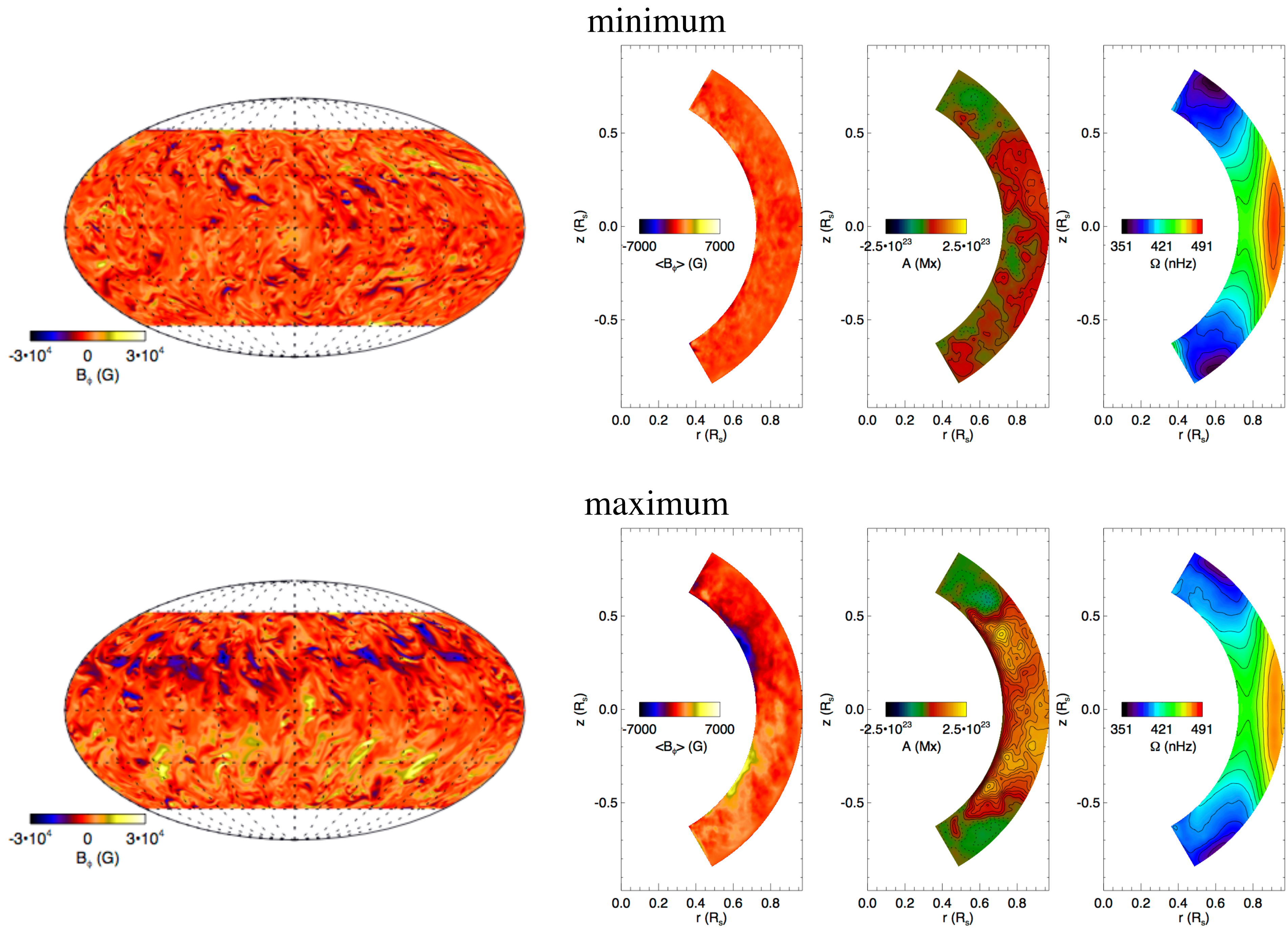

minimum
maximum
-3•10^4
0
3•10^4
B_ϕ (G)
-7000
7000
<B_ϕ> (G)
-2.5•10^23
2.5•10^23
A (Mx)
351
421
491
Ω (nHz)
z (R_s)
r (R_s)
0.5
0.0
-0.5
0.0 0.2 0.4 0.6 0.8

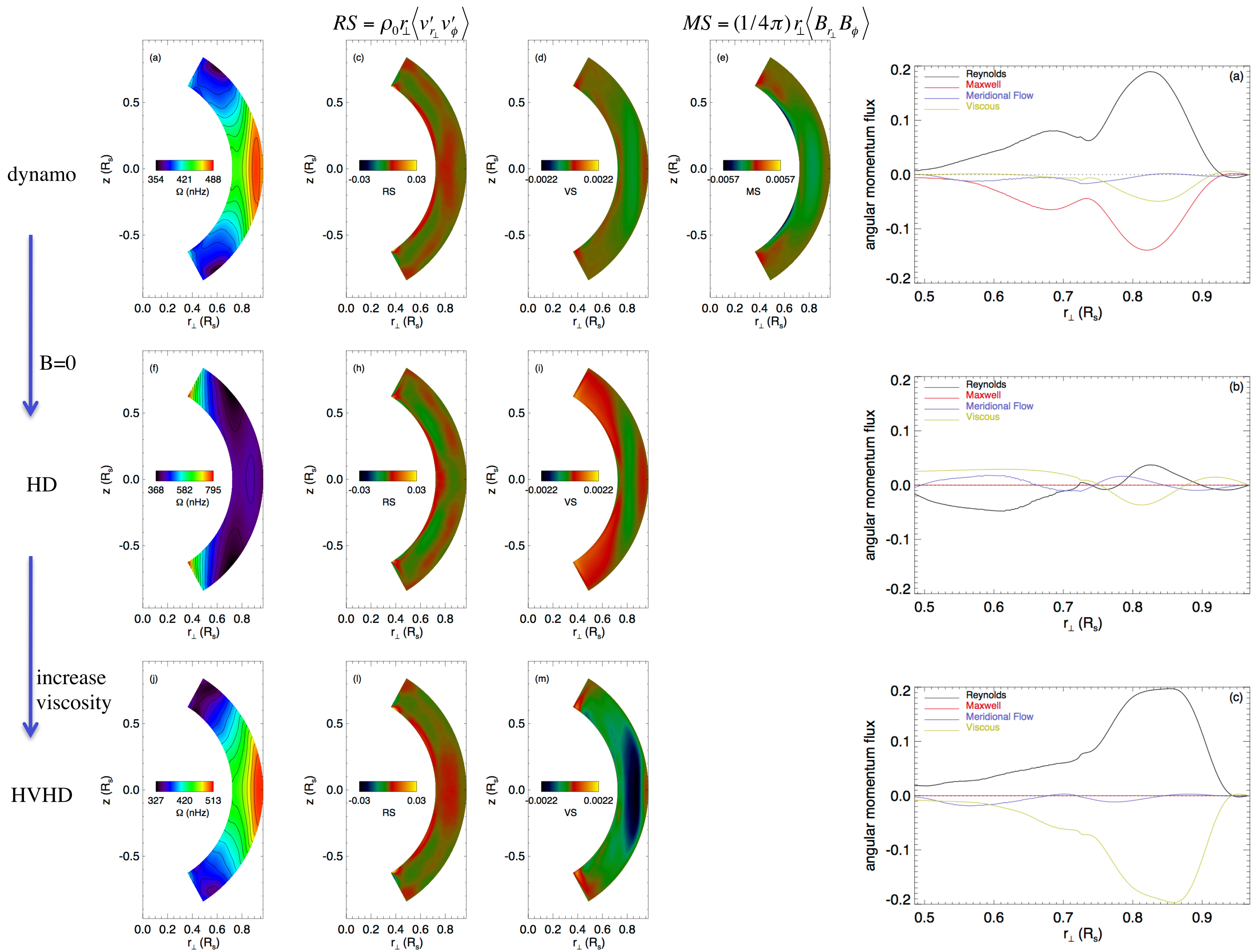

$RS = \rho_0 r_\perp \langle v'_{r_\perp} v'_\phi \rangle$
$MS = (1/4\pi) r_\perp \langle B_{r_\perp} B_\phi \rangle$
dynamo
B=0
HD
increase viscosity
HVHD
(a)
354 421 488
Ω (nHz)
(c)
-0.03 0.03
RS
(d)
-0.0022 0.0022
VS
(e)
-0.0057 0.0057
MS
(f)
368 582 795
Ω (nHz)
(h)
-0.03 0.03
RS
(i)
-0.0022 0.0022
VS
(j)
327 420 513
Ω (nHz)
(l)
-0.03 0.03
RS
(m)
-0.0022 0.0022
VS
z (Rs)
r⊥ (Rs)
angular momentum flux
Reynolds
Maxwell
Meridional Flow
Viscous
(a)
(b)
(c)

- **Transition between solar-like and anti-solar differential rotation takes place at *Ro* ~ 1:**

Gastine et al. (2014)

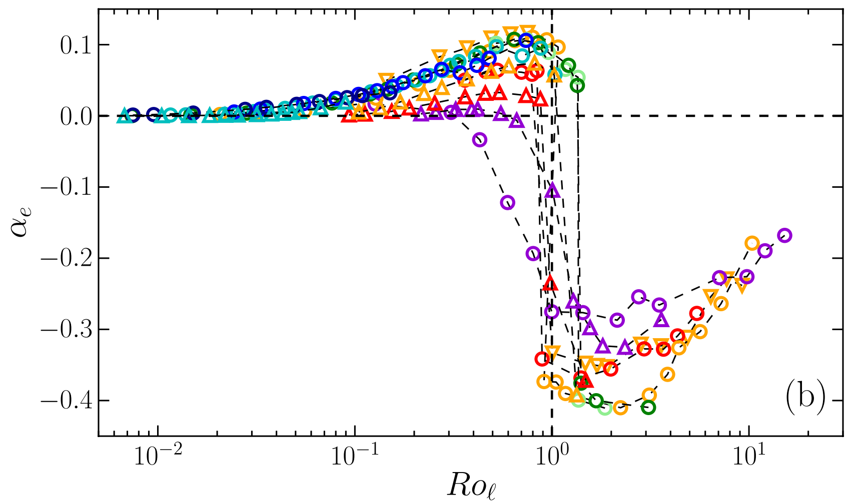

- **Presence of the magnetic field suppresses convection, making the flow more rotationally constrained, and changes the Reynolds stress transport of angular momentum:**

$$Ro = u_{rms,all} / \Omega H_p$$

dynamo: $Ro = 0.74$ HD: $Ro = 0.96$ HVHD: $Ro = 0.71$

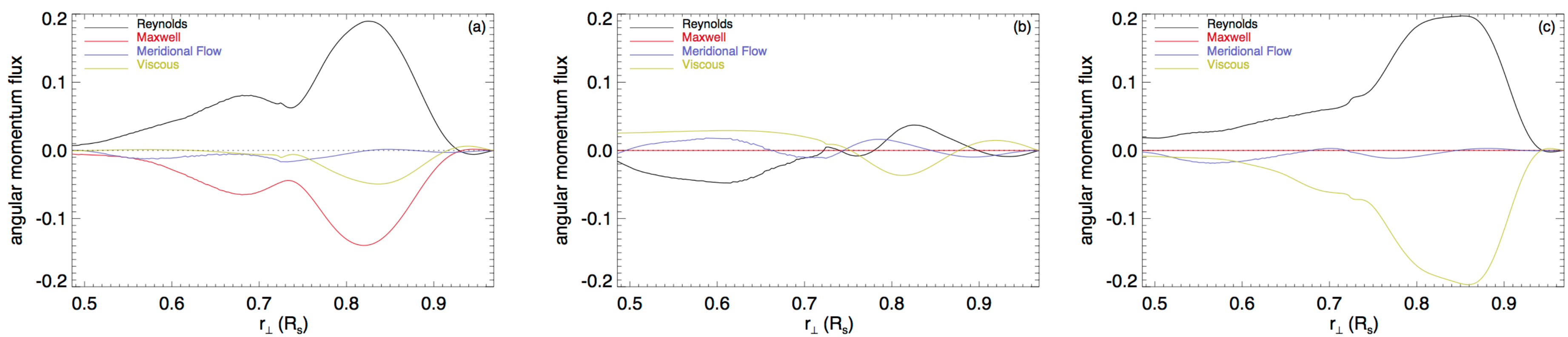

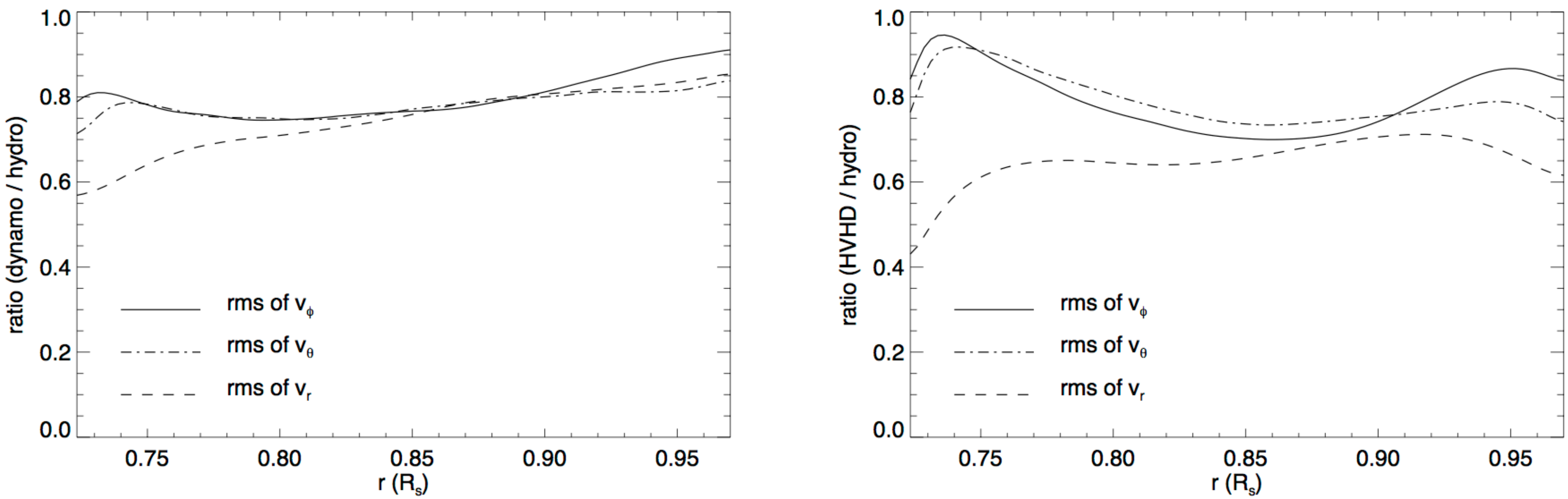

ratio (dynamo / hydro)
rms of v_ϕ
rms of v_θ
rms of v_r
r (R_s)
ratio (HVHD / hydro)
rms of v_ϕ
rms of v_θ
rms of v_r
r (R_s)

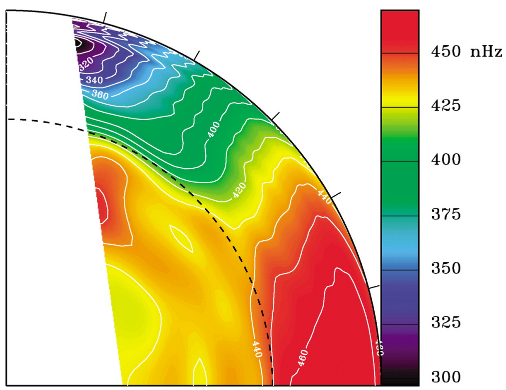
450 nHz
425
400
375
350
325
300

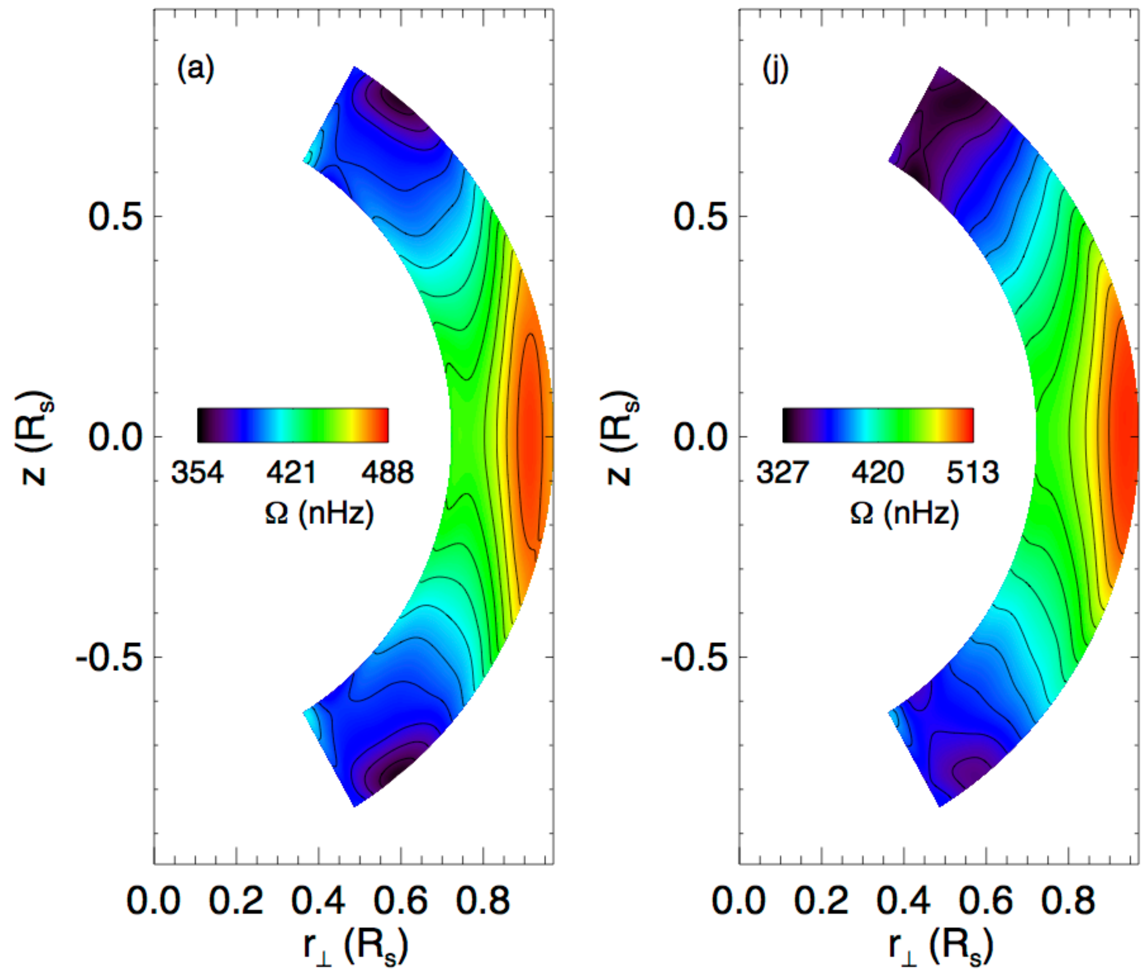
(a)
(j)
0.5
0.0
-0.5
z (Rs)
354
421
488
327
420
513
Ω (nHz)
0.0
0.2
0.4
0.6
0.8
r⊥ (Rs)

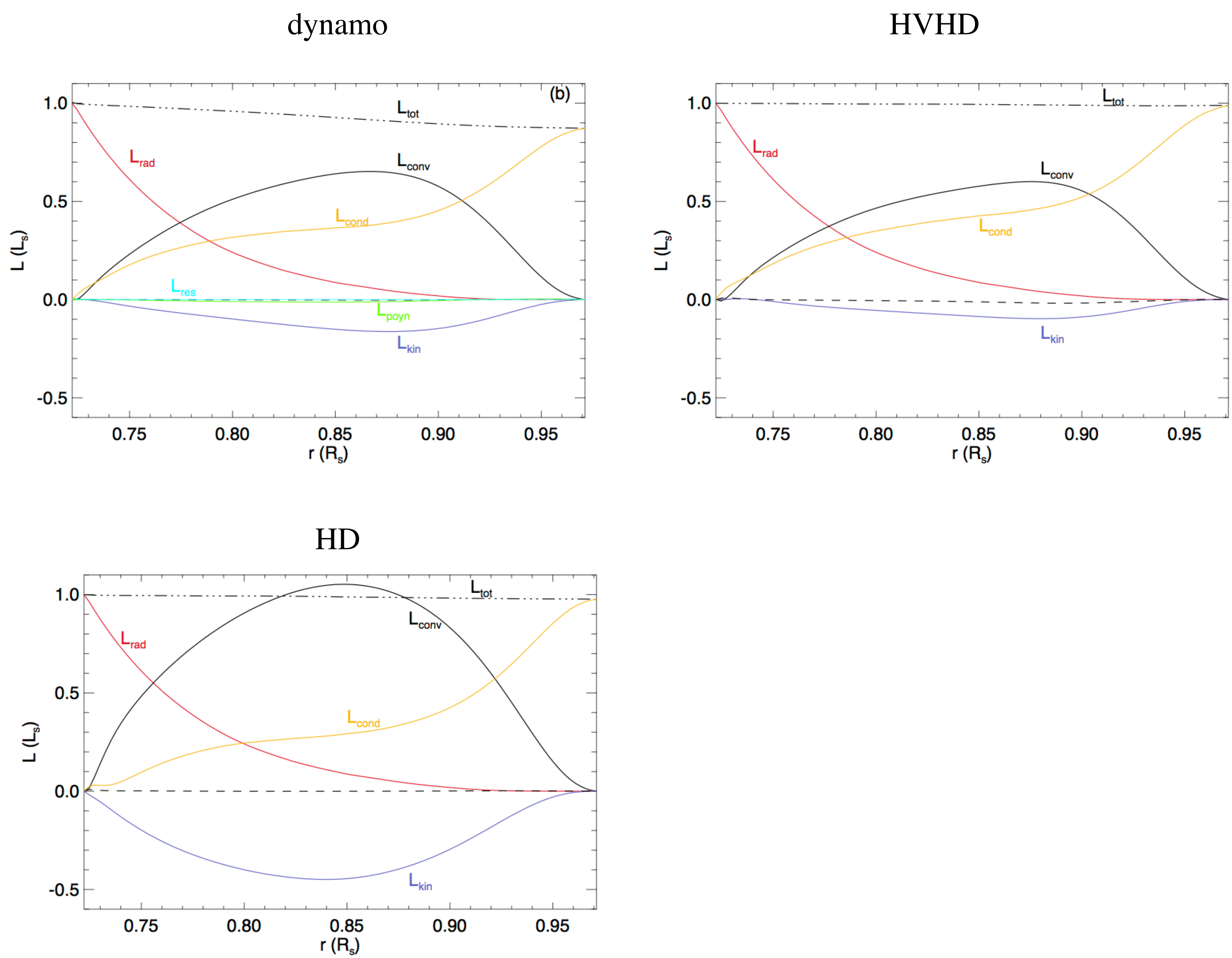
dynamo
HVHD
HD
(b)
L (Ls)
r (Rs)
Ltot
Lrad
Lconv
Lcond
Lres
Lpoyn
Lkin
1.0
0.5
0.0
-0.5
0.75
0.80
0.85
0.90
0.95

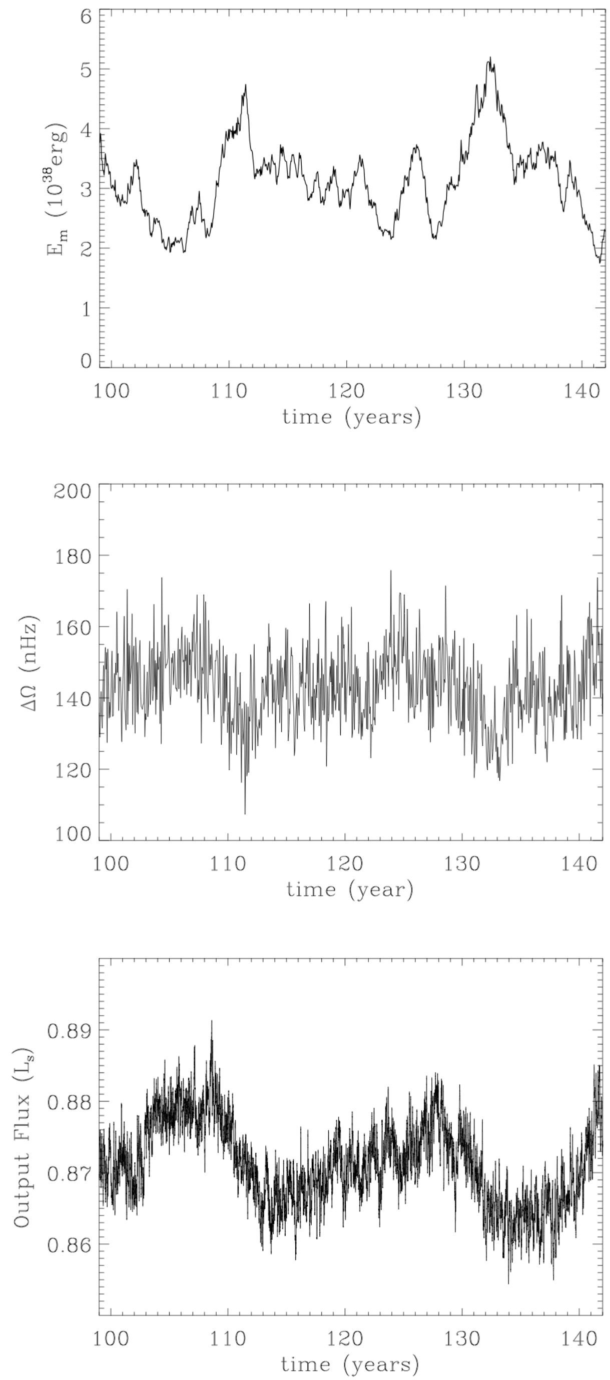
E_m (10^{38}erg)
time (years)
ΔΩ (nHz)
time (year)
Output Flux (L_s)
time (years)

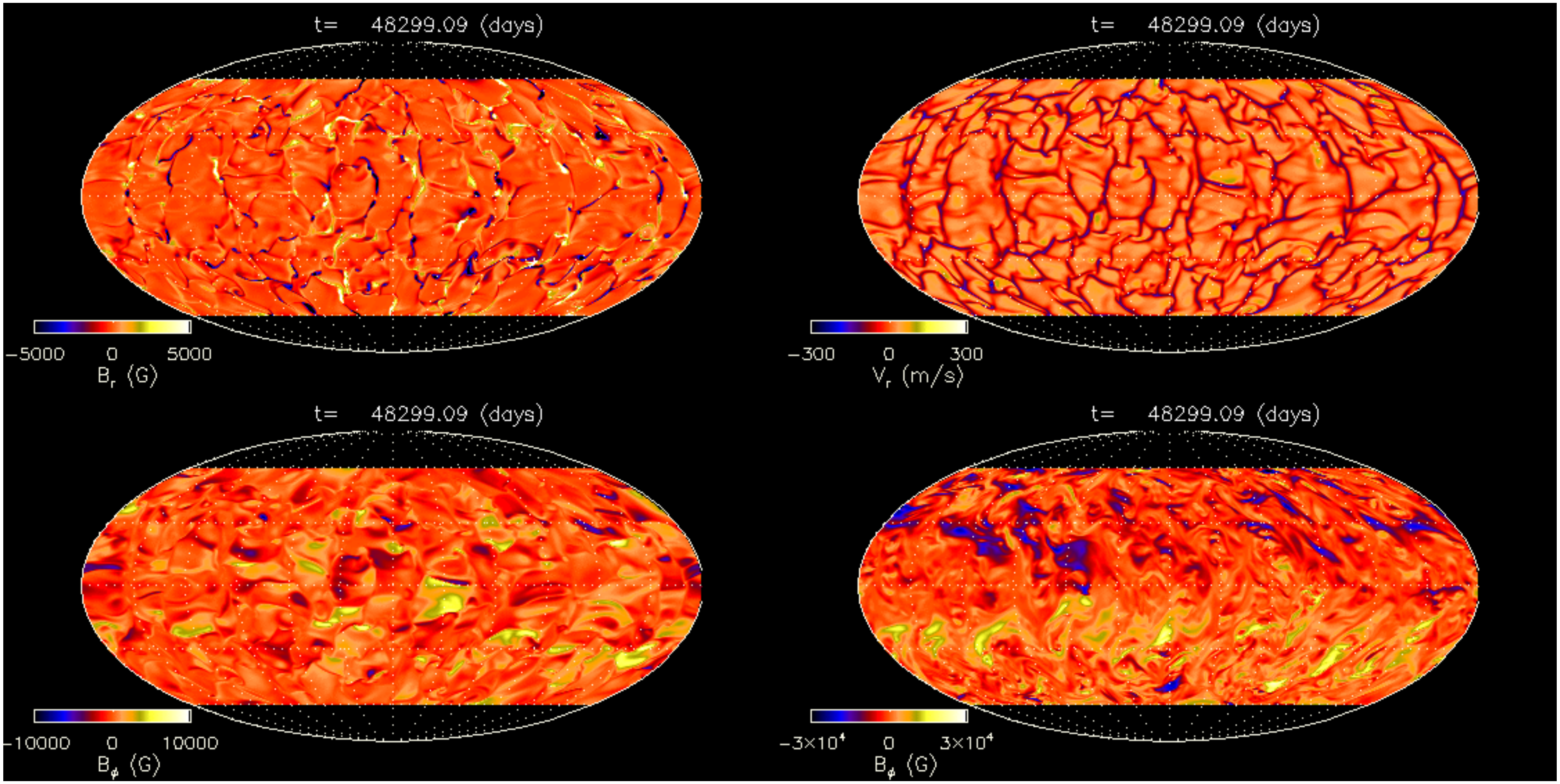
t= 48299.09 (days)
-5000 0 5000
B_r (G)
t= 48299.09 (days)
-300 0 300
V_r (m/s)
t= 48299.09 (days)
-10000 0 10000
B_ϕ (G)
t= 48299.09 (days)
-3×10^4 0 3×10^4
B_ϕ (G)

Examples of strong flux emergence events

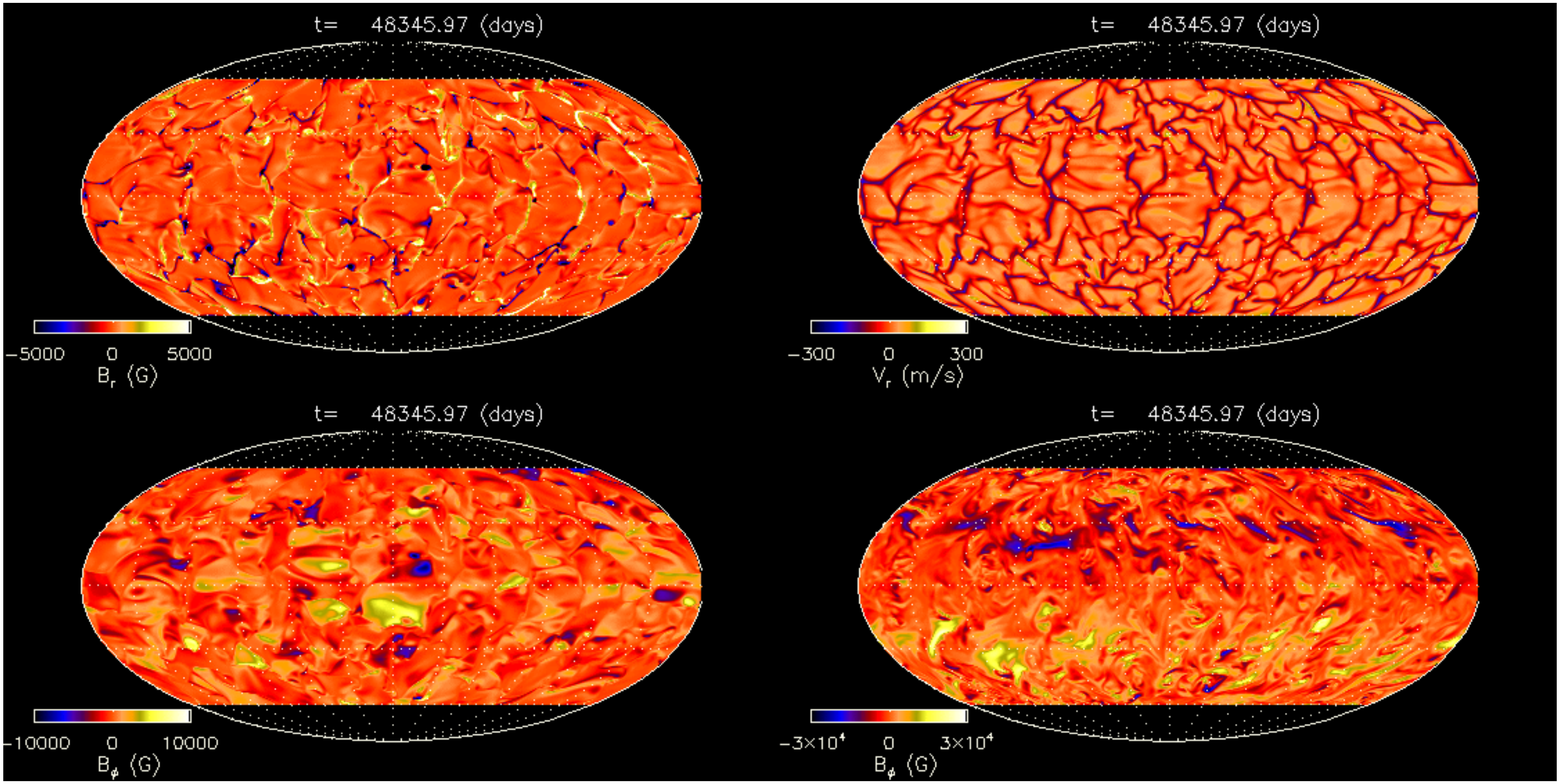

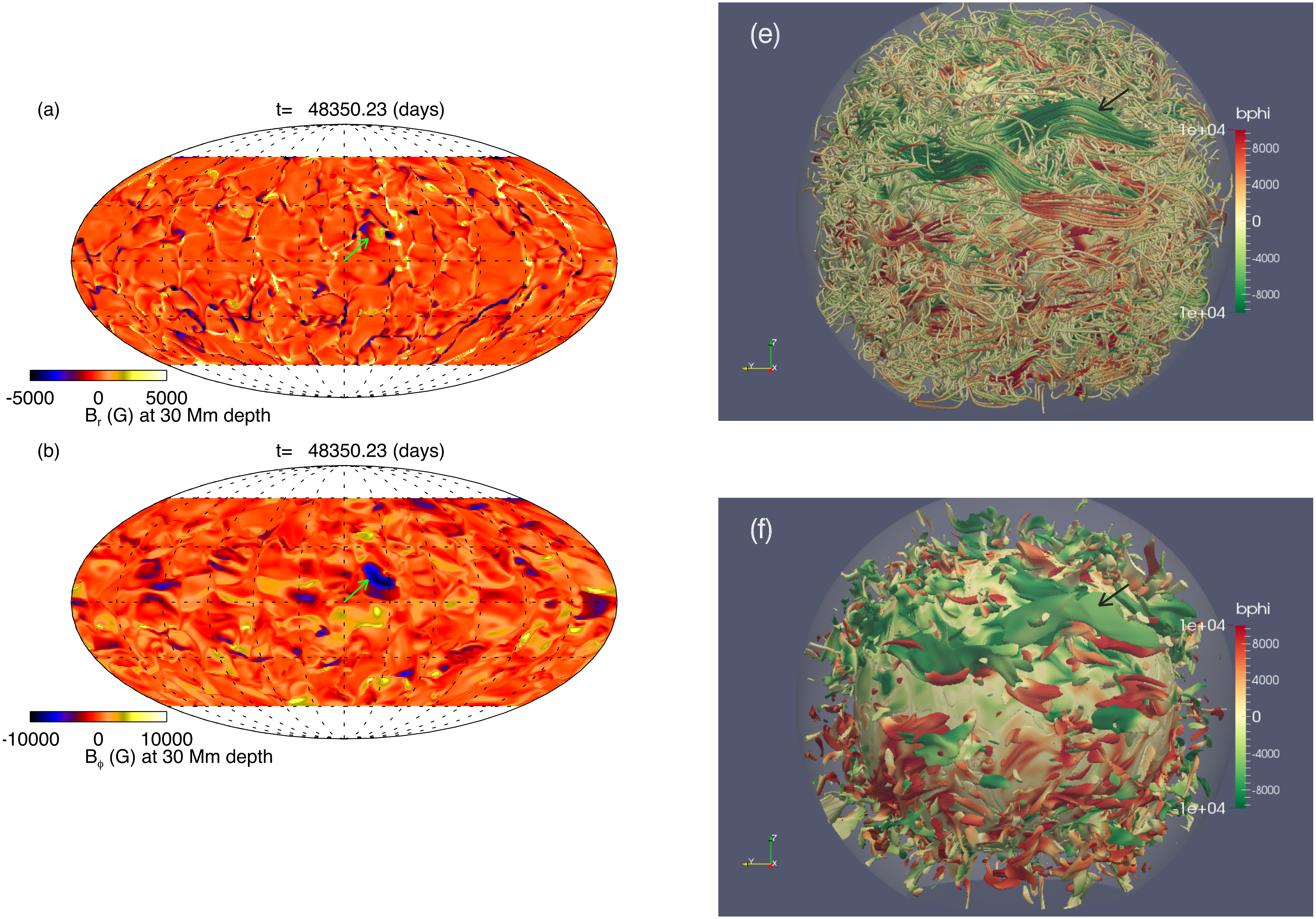
(a)
t= 48350.23 (days)
-5000
0
5000
B_r (G) at 30 Mm depth
(b)
t= 48350.23 (days)
-10000
0
10000
B_ϕ (G) at 30 Mm depth
(e)
bphi
1e+04
8000
4000
0
-4000
-8000
-1e+04
(f)
bphi
1e+04
8000
4000
0
-4000
-8000
-1e+04

• Tilt angles of super-equipartition flux emergence areas at 0.957 R_s:

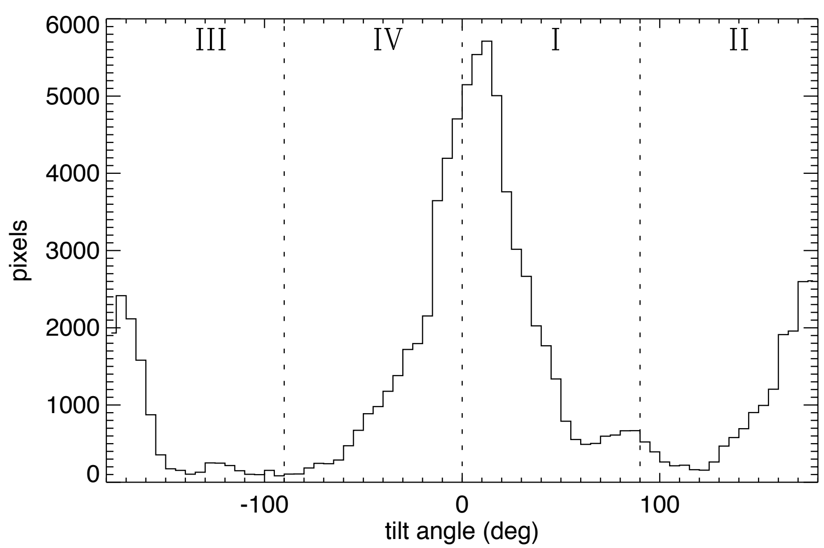

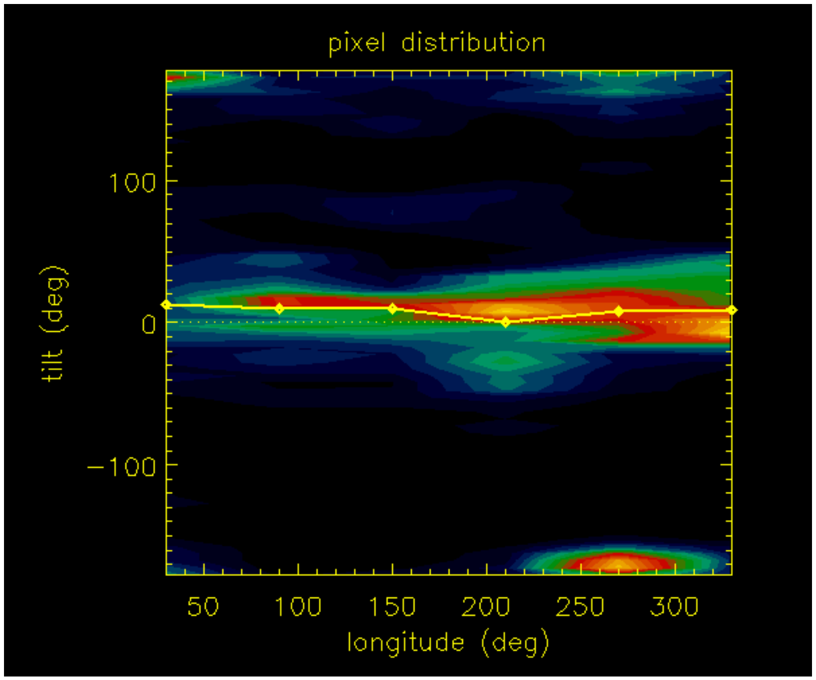

- Conform to Hale's rule by 2.4 to 1 in area
- Statistically significant mean tilt angle: 7.5° ± 1.6°

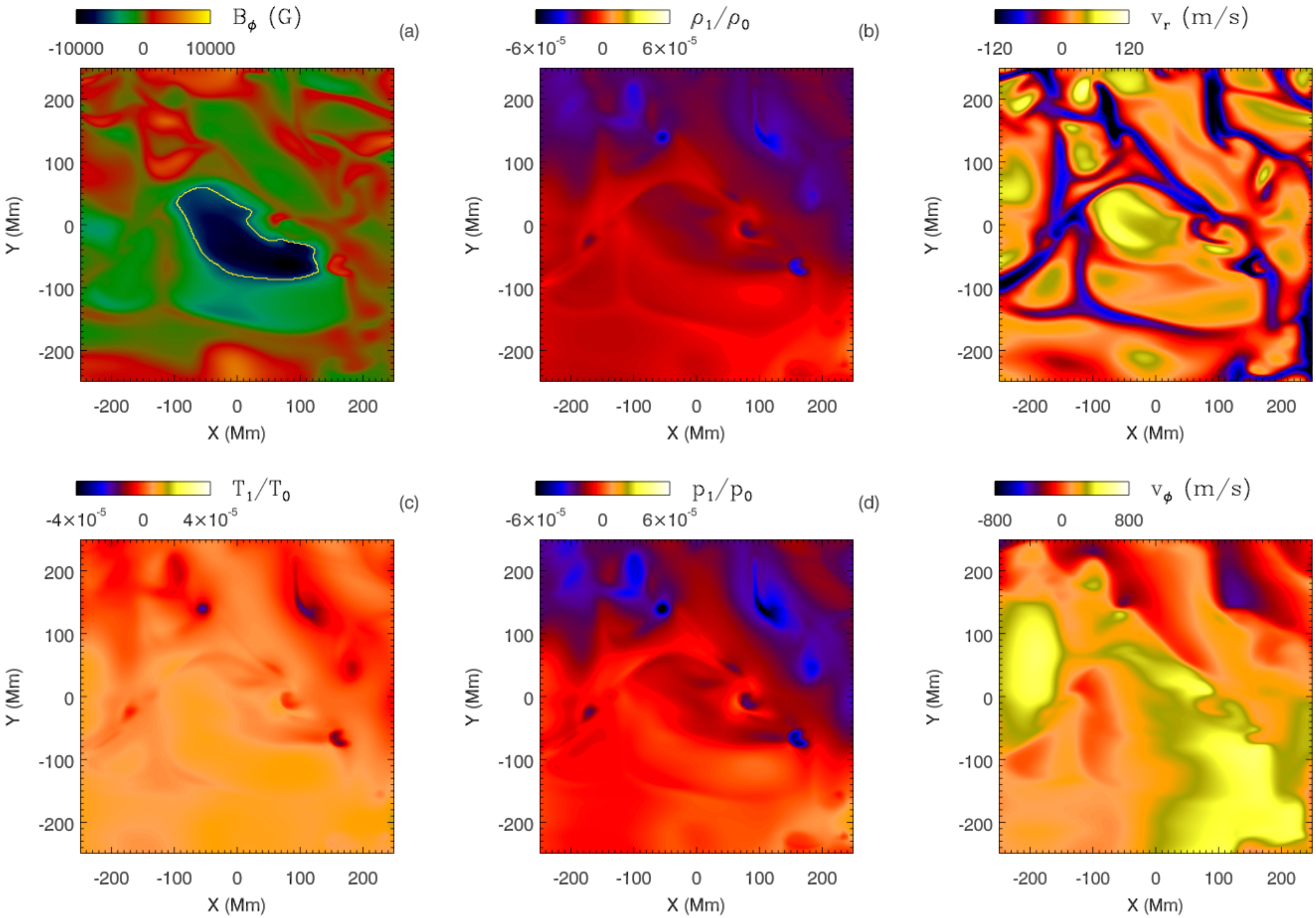

$$\left\langle \rho_1 / \rho_0 \right\rangle \approx -1.6 \times 10^{-5},\ \left\langle p_1 / p_0 \right\rangle \approx -1.1 \times 10^{-5},\ \left\langle T_1 / T_0 \right\rangle \approx 0.5 \times 10^{-5}$$

$$\left\langle V_\phi \right\rangle \approx 129 \text{ m/s relative to mean zonal velocity of the latitude } (15^\circ)$$

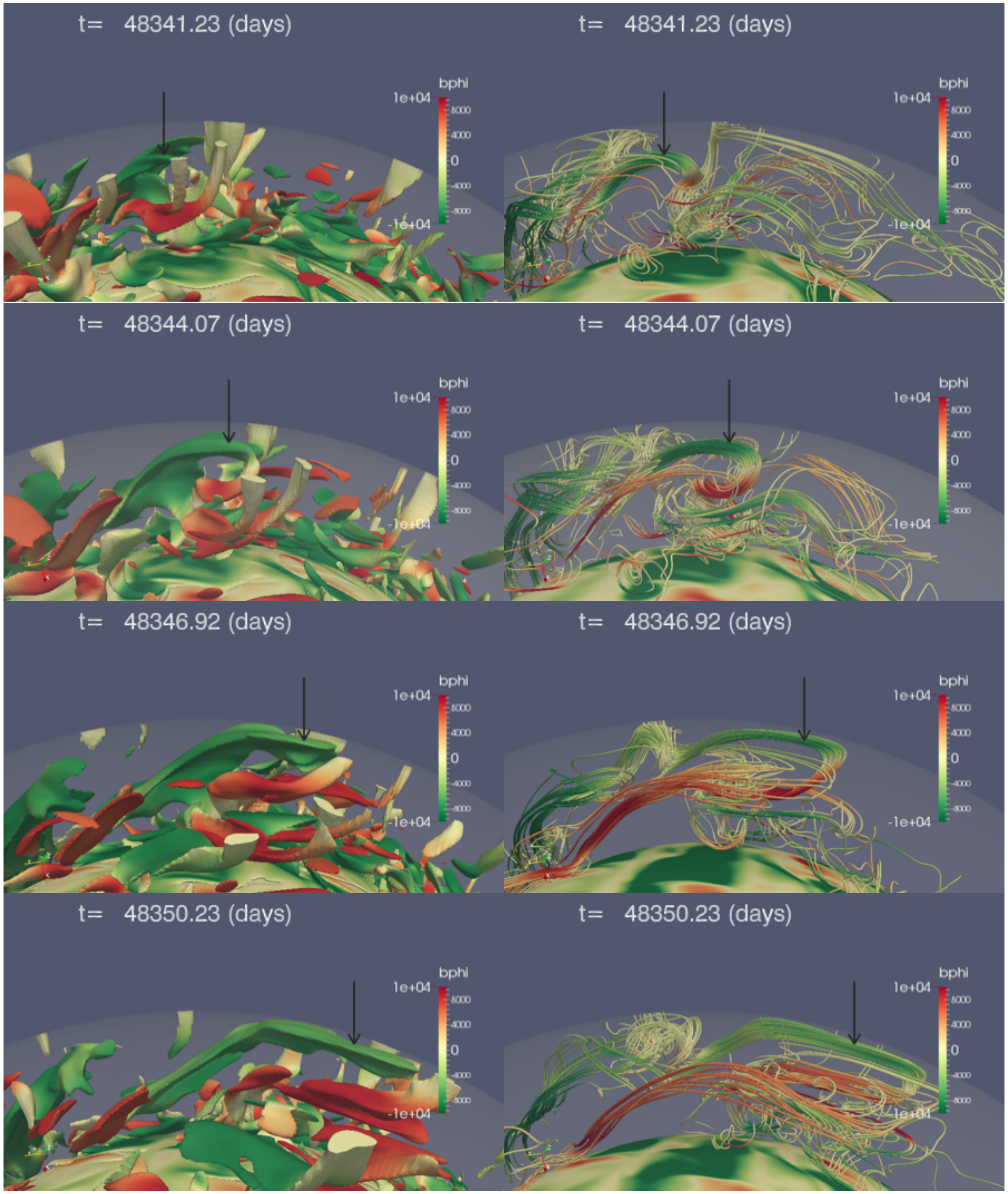
t= 48341.23 (days)
bphi
1e+04
0
-1e+04
t= 48344.07 (days)
t= 48346.92 (days)
t= 48350.23 (days)

- Simulation with further reduced magnetic diffusivity and viscosity, but the same thermal diffusion: $K = 3\times10^{13}\ cm^2 s^{-1}$ at top and decrease with depth as $1/\sqrt{\rho}$, $\eta = 0$, $\nu = 0$.

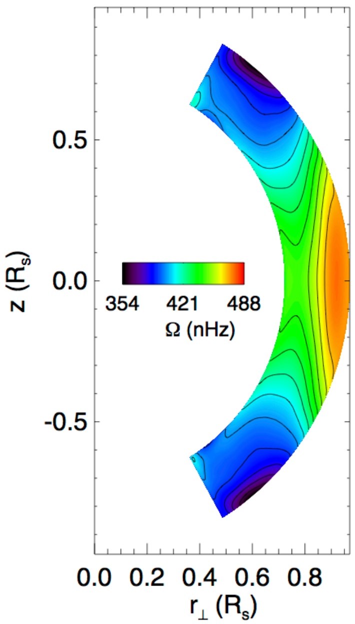

Fan and Fang (2014)

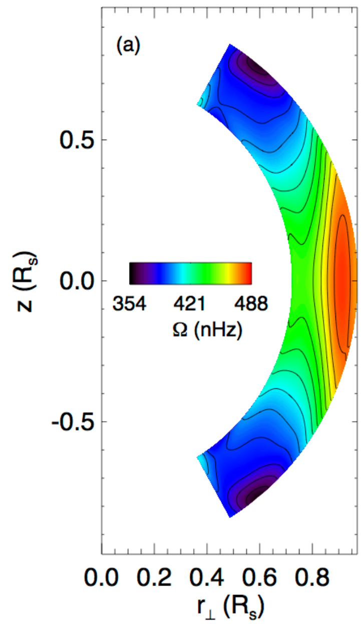

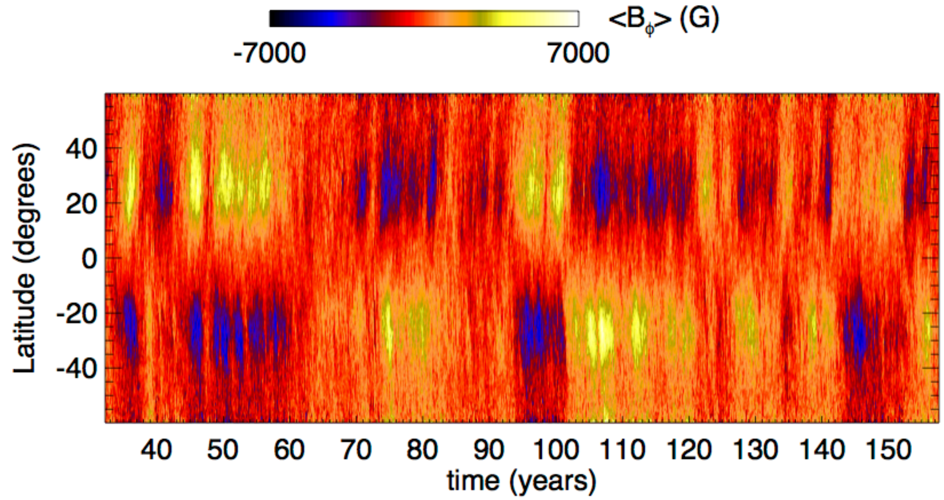

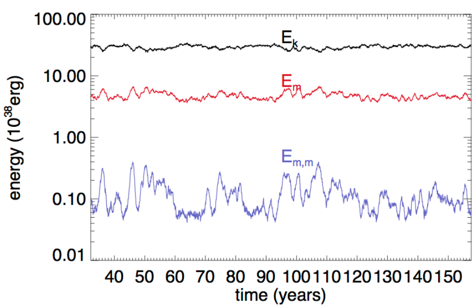

Fan and Fang (2014)

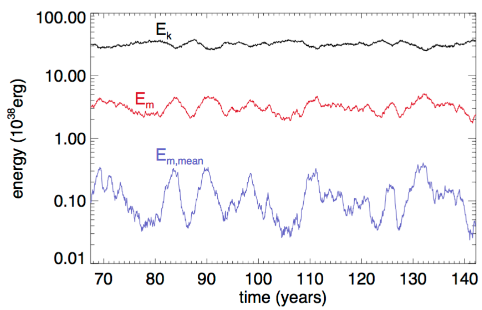

Fan and Fang (2014)

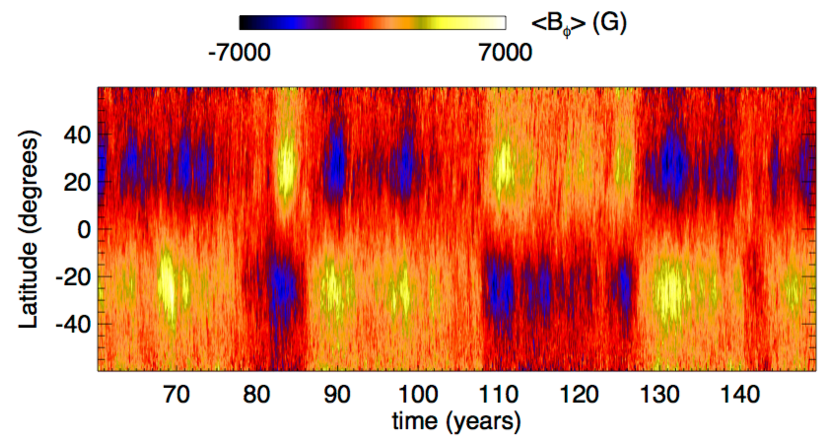

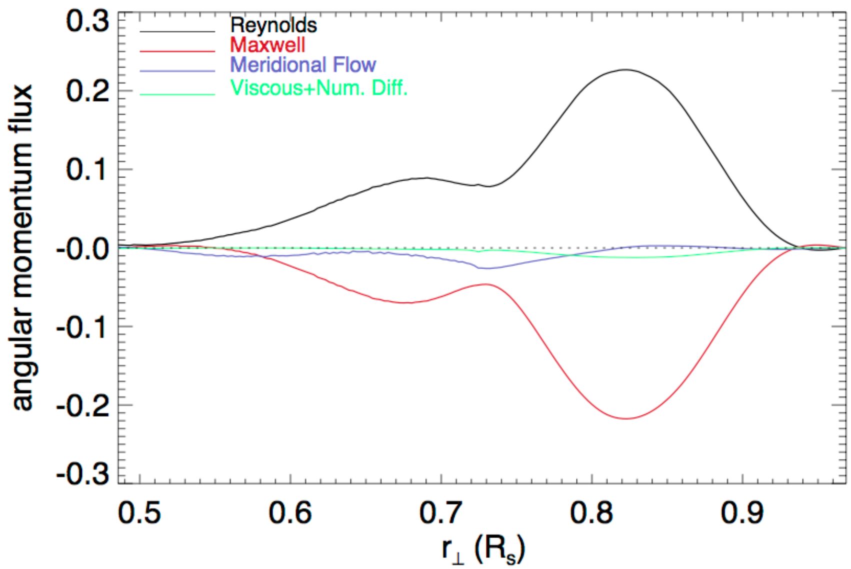

Fan and Fang (2014)

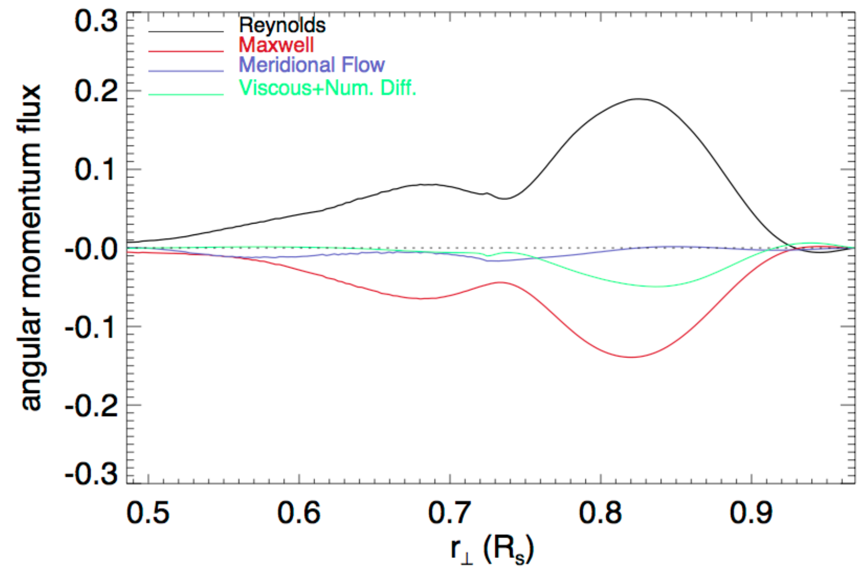

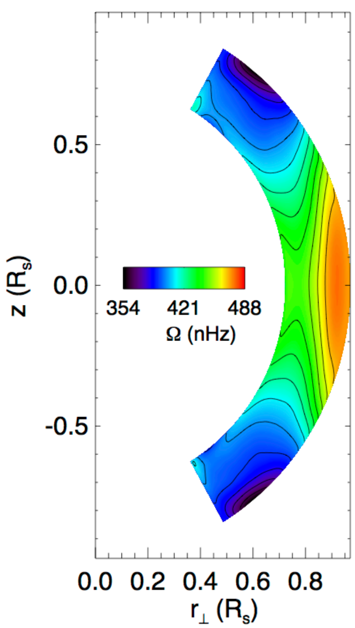

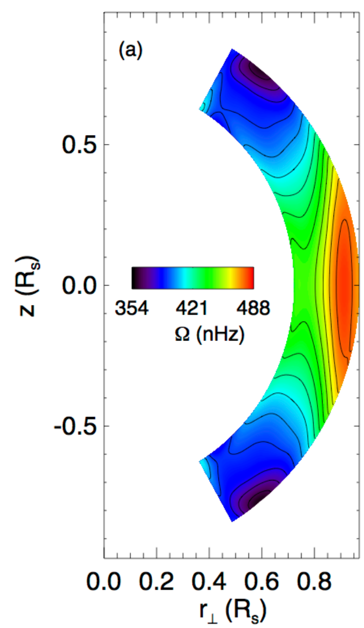

Summary

- A 3D convective dynamo in the rotating solar convective envelope driven by the radiative heat flux produces a large-scale mean magnetic field that exhibits irregular cyclic behavior with oscillation time scales ranging from about 5 to 15 years and undergoes irregular polarity reversals. This result seems to be robust with further reduced magnetic diffusivity and viscosity

- The mean axisymmetric toroidal magnetic field peaks at the bottom of the convection zone, reaching a value of about 7000 G. Including the fluctuating component, individual channels of strong field reaching 30kG are present.

- The presence of the magnetic fields plays an important role in the self-consistent maintenance of the solar-like differential rotation. In several ways acts like an enhanced viscosity:
  - Suppress large scale convection (more suppression of v_r), make it more rotationally constrained $\rightarrow$ outward transport of angular momentum by the Reynolds stress.
  - Take up the main role of balancing the Reynolds stress transport with the Maxwell stress transport.
  - Reduce the downward kinetic energy energy flux

- In the midst of magneto-convection, we found occasional emergence of strong super-equipartition toroidal flux bundles near the surface, exhibiting properties that are similar to emerging solar active regions. They are not rising in isolation from the bottom of the CZ, but are product of continued reconnection and shear amplification by local flows in the bulk of CZ.